Published in final edited form as:
J Biotechnol. 2010 November ; 150(3): 417–427. doi:10.1016/j.jbiotec.2010.09.955.

A putative role for platelet-derived PPARγ in vascular homeostasis demonstrated by anti-PPARγ induction of bleeding, thrombocytopenia and compensatory megakaryocytopoiesis

Patricia J. Simpson-Haidaris[1,2,3,*], **Kathryn E. Seweryniak**[4], **Sherry L. Spinelli**[3], **Tatiana M. Garcia-Bates**[2], **Thomas I. Murant**[4], **Stephen J. Pollock**[4], **Patricia J. Sime**[1], and **Richard P. Phipps**[4]

[1]Department of Medicine, University of Rochester School of Medicine and Dentistry 601 Elmwood Ave Rochester, NY 14642 USA

[2]Department of Microbiology and Immunology, University of Rochester School of Medicine and Dentistry 601 Elmwood Ave Rochester, NY 14642 USA

[3]Department of Pathology and Laboratory Medicine, University of Rochester School of Medicine and Dentistry 601 Elmwood Ave Rochester, NY 14642 USA

[4]Department of Environmental Medicine University of Rochester School of Medicine and Dentistry 601 Elmwood Ave Rochester, NY 14642 USA

Abstract

Widely known for its role in adipogenesis and energy metabolism, PPARγ also plays a role in platelet function. To further understand functions of platelet-derived PPARγ, we produced rabbit polyclonal (PoAbs) and mouse monoclonal (MoAbs) antibodies against PPARγ 14mer/19mer peptide-immunogens. Unexpectedly, our work produced two key findings. First, MoAbs but not PoAbs produced against PPARγ peptide-immunogens displayed antigenic crossreactivity with highly conserved PPARα and PPARβ/δ. Similarly, Santa Cruz PoAb sc-7196 was monospecific for PPARγ while MoAb sc-7273 crossreacted with PPARα and PPARβ/δ. Second, immunized rabbits and mice exhibited unusual pathology including cachexia, excessive bleeding, and low platelet counts leading to thrombocytopenia. Spleens from immunized mice were fatty, hemorrhagic and friable. Although passive administration of anti-PPARγ PoAbs failed to induce experimental thrombocytopenia, megakaryocytopoiesis was induced 4–8–fold in mouse spleens. Similarly, marrow megakaryocytopoiesis was enhanced 1.8–4–fold in immunized rabbits. These peptide-immunogens are 100% conserved in human, rabbit and mouse; thus, immune-mediated platelet destruction via crossreactivity with platelet-derived PPARγ likely caused bleeding, thrombocytopenia, and compensatory megakaryocytopoiesis. Such overt pathology would cause significant problems for large-scale production of anti-PPARγ PoAbs. Furthermore, a major pitfall

[*]**Address all correspondence to:** P.J. Simpson-Haidaris, Ph.D., Department of Medicine, Hematology-Oncology Division, P.O. Box 704, 601 Elmwood Ave., Rochester, NY 14642. TEL: 585-275-8267; FAX 585-273-1042; pj_simpsonhaidaris@urmc.rochester.edu..

Author Contributions to the Work:

PJS-H developed the concept, designed and performed experiments, analyzed data, prepared figures and wrote the manuscript; KES designed and performed experiments, analyzed data and edited the paper; SLS, TMG-B, TIM, and SJP performed experiments and edited the manuscript; PJS and RPP made substantial contributions to interpretation of the data, critical revisions to the manuscript for important intellectual content and supplied critical reagents.

associated with MoAb production against closely related molecules is that monoclonicity does not guarantee monospecificity, an issue worth further scientific scrutiny.

Keywords

Monoclonal Antibody Production; MAP Technology; Thrombocytopenia; Megakaryocytopoiesis; Peroxisome Proliferator-Activated Receptors; Platelets

1. Introduction

Ligand-activated peroxisome proliferator-activated receptor (PPAR) transcription factors are members of the largest subclass of the nuclear hormone receptor superfamily (Michalik et al., 2006). PPARs regulate target genes participating in pathways of glucose and lipid metabolism, adipogenesis, and inflammation. They share a high degree of structural homology in the DNA-, ligand- and cofactor-binding domains with all members of the superfamily (Michalik et al., 2006). Transcriptional regulation by PPARs requires dimerization with the retinoid-X-receptor (RXR) and binding of the heterodimer to its cognate response element in the promoter region of target genes (Michalik et al., 2006). Three isoforms, PPARα , PPARβ/δ, and PPARγ, encoded by separate genes have been identified, and variants of each major isoform exist due to alternative promoter usage and/or alternative processing of the primary RNA transcripts (Gervois et al., 1999, Larsen et al., 2002, Garcia-Bates et al., 2008b). Whereas, PPARα and PPARγ exhibit some tissue-selectivity in expression, the PPARβ/δ isoform is ubiquitously expressed. The conservation in primary structure of the PPAR family members (α, β/δ, and γ) is high both within and across species. Furthermore, PPARγ is expressed as two major isoforms, γ1 and γ2, of which PPARγ2 is found at high levels in adipose tissue (Tontonoz and Spiegelman, 2008).

Megakaryocytes and platelets express PPARγ (Akbiyik et al., 2004), and recently we reported that PPARγ1 is released from activated platelets and in platelet microparticles as an active transcription factor complex with RXR (Ray et al., 2008). Internalization of PPARγ-containing platelet microparticles elicits a transcellular attenuation of THP-1 monocytic cell activation in the presence of the PPARγ agonist, rosiglitazone (Ray et al., 2008). PPARγ activation exerts anti-inflammatory effects in nucleated cells via nongenomic mechanisms (Ray et al., 2006). Other transcription factors are found in anucleate platelets including PPARβ/δ (Ali et al., 2006), RXR (Moraes et al., 2007), Stat3 (Vassilev et al., 2002), glucocorticoid receptor (Moraes et al., 2005), and NF-κB family members (Liu et al., 2002, Spinelli et al., 2010). However, the mechanisms by which platelet-derived nuclear receptors regulate nongenomic functions during thrombosis, metabolism or inflammation are poorly understood.

To further elucidate the function(s) of PPARγ released during platelet activation and in platelet microparticles, we produced rabbit polyclonal (PoAbs) and mouse monoclonal (MoAbs) antibodies against PPARγ synthetic peptides. Although a number of anti-PPARγ antibodies are commercially available, we chose to produce our own because two commercially available PoAbs used previously (Feldon et al., 2006, Ray et al., 2008, O'Brien et al., 2008) became unavailable. Furthermore, according to the product specification sheets, these antibodies could not be used for Western immunodetection in the presence of serum albumin, hence prohibiting their use for detection of PPARγ in blood-derived platelets. Herein, we report the unexpected and remarkable pathology associated with the production of both rabbit PoAbs and mouse MoAbs against human PPARγ1 and PPARγ2, including cachexia and induction of thrombocytopenia and megakaryocytopoiesis,

as well as the lack of isoform specificity of anti-PPARγ MoAbs produced by us and one commercial MoAb that is widely used in the literature.

2. Materials and methods

2.1. Animals and cell lines

Two–three–month-old female New Zealand white rabbits (RSI, Mocksville, NC) were purchased for production of PoAbs against PPARγ synthetic peptides. Six–eight–week-old Balb/c female mice were acquired from Jackson (JAX) Laboratory (Bar Harbor, ME) for immunization and harvest of sensitized spleens for hybridoma production. Retired Balb/c female breeders (JAX or Charles Rivers, Wilmington, MA) were used for production of MoAb in ascites fluid. Animal protocols were approved by the University of Rochester's Committee on Animal Resources (UCAR) and conform to state and federal guidelines. P3X63-AG8.653 parental myeloma cells were obtained from the ATCC (Manassas, VA) and used as the hybridoma fusion partner. Myeloma cells were grown in Excell 610 HSF medium (Sigma-Aldrich, St. Louis, MO) supplemented with 2 mM L-glutamine, 100 Units/ml penicillin and 100 μg/ml streptomycin (Invitrogen, Carlsbad, CA) and 5-10% heat-inactivated FBS (Hyclone, Thermo Fisher, Rockford, IL). Hybridoma selection medium was supplemented with 1X HAT (Invitrogen or Sigma).

2.2. Peptide-immunogens

To generate antibodies that would recognize both human and mouse PPARγ1/2, but not interfere with known functions of PPARγ, we chose sequences for peptide-immunogens from the PPARγ1 primary structure (NP_619726) that were 100% identical between human and mouse. The following criteria based on our experience (Simpson-Haidaris et al., 1989a, Simpson-Haidaris et al., 1989b, Fay et al., 1991) were applied to the design of peptide-immunogens: 1) the density of charged amino acids (R/K/D/E) for enhanced aqueous solubility; 2) the presence of at least one proline residue to restrict conformational presentation; (3) the absence of cysteine residues to prevent disulfide exchange; 4) an α-helical structure or surface exposed region based on crystal structure determinations; 5) a linear length between 10-20 residues; and 6) the lowest similarity to the primary structure of PPARα and PPARβ/δ.

Two peptides were chosen for antibody production, a 14mer corresponding to residues 239-GKTTDKSPFVIYDM-252 and a 19mer corresponding to residues 253-NSLMMGEDKIKFK HITPLQ-271 of the PPARγ1 primary structure, according to protein database accession #NP_619726. The peptides were custom synthesized and coupled to MAP (Multiple Antigen Peptide) carriers by Quality Controlled Biochemicals (Hopkinton, MA). Additional peptides were synthesized for epitope mapping by ELISA and include: 1) free 14mer, GKTTDKSPFVIYDM; 2) scrambled 14mer, VDGKKMISTYDIPV; 3) NH_2-terminal 14mer, GKTTDKSP; 4) COOH-terminal 14mer, SPFVIYDM; and 5) COOH-terminal 19mer, DKIKFKHITPLQ.

2.3. Immunization, test bleeding and hybridoma fusion

Rabbits—Two rabbits were used for each MAP-peptide-immunogen. The rabbits were allowed to acclimate to their new environment for 12 days then pre-immune serum was collected. The MAP-peptide-immunogens were dissolved in PBS at 4 mg/ml and diluted accordingly in PBS to the desired concentration for emulsification with adjuvants. For the primary immunization, rabbits were injected with 2 mg MAP-peptide-immunogen emulsified in Complete Freund's Adjuvant (CFA) delivered subcutaneously to four sites (0.25 ml/site) along the dorsal aspect and between the scapulae spaced 3–4 cm apart. Six booster injections consisting of 350-750 μg peptide-immunogen emulsified in Incomplete

Freund's Adjuvant (IFA) were delivered over four new sites every four weeks. Two control rabbits were mock-immunized with emulsions of adjuvant and PBS following a similar schedule. Test bleeds were performed under mild sedation 10-17 days after each booster injection. Final bleeds were obtained via intracardiac puncture, whereby rabbits were deeply sedated; intravenous delivery of 1 ml sodium pentobarbital (390 mg/ml) followed to ensure euthanasia. Rabbit IgG fractions were prepared by 45% ammonium sulfate precipitation of serum followed by dialysis in PBS. Purified rabbit IgG was prepared by Protein-A affinity chromatography (Andrew and Titus, 2001). Rabbit blood chemistries, CBC with cell differentials and platelet counts were performed by VetCheck Laboratory, Inc (Farmington, NY).

Mice—Three mice were used for each MAP-peptide-immunogen. Prebleed and test bleed sera were obtained by submandibular bleed. For the primary immunization, each mouse was injected IP with 175 μg MAP-peptide-immunogen emulsified in CFA. Two or three booster injections were given alternating with either MAP-peptide-immunogen (50-200 μg) emulsified in IFA delivered IP or 50 μg peptide-immunogen in 100 μl PBS delivered IV in the lateral tail vein. A final boost of 50 μg peptide-immunogen in 100 μl PBS was delivered IV three days prior to aseptically harvesting the spleen. Final bleeds were obtained by intracardiac puncture under CO_2 sedation, followed by euthanasia for spleen harvest. Spleen cells were fused with the parent myeloma cell line following standard protocols for hybridoma and ascites fluid production as previously reported (Simpson-Haidaris et al., 1989a, Simpson-Haidaris et al., 1989b, Fay et al., 1991), except that PEG 4000 was obtained from the ATCC.

2.4. ELISA and Western blot immunodetection

Immulon 4-HBX microtiter plates (Dynex Technologies/VWR) were used for binding synthetic peptide antigens for ELISA. The pMAL™ Protein Fusion and Purification System from New England Biolabs was used to prepare recombinant PPARγ1 protein. PPARγ1 cDNA was subcloned into the pMAL-2pE expression vector, which directs expression of recombinant human PPARγ1 fused to the maltose binding protein (MBP) in the periplasmic space in *E. coli*. Periplasmic MAP-rPPARγ1 fusion protein was isolated by the cold osmotic shock procedure per kit instructions. Test bleeds from immunized rabbits and mice and tissue culture supernatants from the primary plating of hybridoma fusions were screened (and hybridomas selected for expansion) by ELISA using dual positive selection criteria. The antigens used for coating ELISA plates were the MAP-peptide 14mer or 19mer immunogens (4 μg/well) or 100 μl of the MBP-rPPARγ1 fusion protein diluted in 0.05 M sodium carbonate coating buffer, pH 9.6. Rabbit bleeds and hybridomas testing positive for both their respective immunogens and the MBP-rPPARγ1 fusion protein by ELISA were selected for further testing by ELISA and immunoblotting against lysates of human tissue and primary cells and purified rPPAR isoforms.

The human tissue and cell lysates from abdominal adipose tissue, platelets, and primary lung and orbital fibroblasts were used as positive controls for Western immunodetection. Protein (20 μg per lane) was prepared in 100 mM Tris-HCl (pH 8.3), 0.1% SDS, 0.5% NP40 (Igepal, Sigma), 0.5% deoxycholate, 1 mM N-ethylmaleimide, 1 mM iodoacetic acid, 2 mM PMSF and 2 mM EDTA supplemented with Protease Inhibitor Cocktail (Sigma). Purified human rPPARα, rPPARβ/δ and rPPARγ1 proteins were obtained from Protein One (Bethesda, MD) and used for ELISA (50 ng/well), and for SDS-PAGE and Western immunodetection at 0.1–1 μg/lane. HRP-conjugated secondary antibodies were from Sigma or Jackson ImmunoResearch (West Grove, PA). Chemiluminescence detection of immunoreactive protein bands was performed using Immobilon Western HRP Substrate (Millipore, Billerica, MA) and x-ray film. Selected hybridomas were rendered monoclonal

by one to two rounds of subcloning by limiting dilution. The isotype of heavy and light immunoglobulin chains was determined using test strips (MMT1) from AbD-Serotec (Oxford, UK/VWR).

2.5. Histology and quantification of bone marrow and spleen megakaryocytes

Organs harvested from rabbits and mice at the time of sacrifice were fixed in formalin, embedded in paraffin, and 4-5 μm sections were mounted on glass slides and stained with hematoxylin and eosin (H&E). To collect bone marrow, femurs were split with a rongeur and the marrow plug scraped into formalin for fixation prior to embedding in paraffin blocks, sectioning and H&E staining as described previously (Courtney et al., 1991). Brightfield micrographs of tissue sections were obtained using a Nikon Eclipse E800 microscope equipped with a Spot CCD digital camera. Rabbit bone marrow and mouse spleen megakaryocytes were quantified by counting the number of megakaryocytes on 7.5 × 10.5 inch color pictures printed from digital images obtained from 13 random low-power fields of each condition. Statistical analysis was performed using paired Student's t-test comparing control to treatment; p-values < 0.05 were considered statistically significant.

2.6. Acute and chronic mouse models of thrombocytopenia

To test for induction of acute thrombocytopenia (60 min and 24 hr post-injection), three female Balb/c mice were used per four treatment groups and two routes of administration (IP and IV, tail vein). Purified IgG (2 μg/g body weight) diluted in sterile PBS was administered IP or IV to the following groups: 1) rat anti-GP1bαR300 (emfret Analytics) as positive control; 2) nonimmune rat C301 IgG (emfret Analytics) as negative control; 3) anti-PPARγ-19mer (Patricia rabbit); and, 4) anti-PPARγ-14mer (Rosita rabbit). Blood was collected in 20 μl EDTA-coated glass capillary tubes by retroorbital eye bleed at 1 and 24 hr post-injection. Complete blood cell counts were obtained immediately after blood collection using a HemaTrue Hematology Analyzer (Heska Corp, Loveland, CO). Chronic thrombocytopenia was induced by retro-orbital injection of 4 μg/g body weight of purified IgG diluted in sterile PBS and delivered every 72 hours to five female Balb/c mice per each of the following groups: 1) as positive control, rabbit anti-rat platelet IgG prepared and purified as previously described (Courtney et al., 1991); 2) as negative control, nonimmune rabbit IgG; 3) anti-PPARγ-19mer (Patricia rabbit); and 4) anti-PPARγ-14mer (Rosita rabbit). Complete blood cell counts were obtained on blood collected on days 1 and 10, which were equivalent to 24 hr after the first and fourth dose of IgG, respectively.

3. Results

3.1. Design of peptide-immunogens

Peptide sequences were chosen from a region mapping to residues 225-290 of PPARγ1 for which crystal structure information was also available. The same residues were used to query protein databases (Altschul et al., 1997). Within this region, residues 239-271 displayed the lowest similarity to corresponding regions of PPARα and PPARβ/δ primary structure. The PPARγ-14mer shares 57.1% identity and 78.6% similarity with PPARα and 50.0% identity and 78.6% similarity with PPARβ/δ. The PPARγ-19mer shares 21.1% identity and 36.8% similarity with PPARα and 15.7% identity and 36.8% similarity with PPARβ/δ. Coincidentally, the NSLMMGEDKIKFKHITPLQ 19mer peptide we chose using our selection criteria for peptide-immunogens corresponds closely to PPARγ peptide-immunogens used for production of rabbit anti-PPARγ antisera by three different vendors. Biomol (Catalog #SA-206) and Calbiochem (Catalog #516555) antisera were produced against a 15-mer peptide, MMGEDKIKFKHITPL, which falls within the primary structure of our 19mer peptide. Millipore (formerly a product of Upstate; Catalog #07-466) produces

an anti-PPARγ rabbit PoAb using a 16-mer peptide, GEDKIKFKHITPLQEQ, which maps closely to the same region.

3.2. Anti-PPARγ peptide polyclonal antibodies are monospecific

Testing of the rabbit sera for reactivity against the peptide-immunogens and rPPARs began after the first boost. The ELISA titers of rabbit antisera against the MAP-peptide-immunogens increased significantly after the fourth boost for all four animals and remained relatively constant after boosts 5 and 6 with the exception of one MAP-19mer immunized rabbit (Penelope, Fig. 1A) whose titer dropped significantly after the 6^{th} boost. To further characterize the anti-PPARα peptide antisera, we performed ELISA and Western blot analyses using purified rPPARα, rPPARβ and rPPARγ1 proteins. The isoform specificity of the rPPARs was confirmed by Western immunodetection using commercially available PoAbs produced against synthetic peptides of PPARα and PPARβ/δ, and a chicken PoAb produced against the first 110 amino acids of human PPARγ1. The results indicate that these commercially available PoAbs do indeed detect their respective rPPAR isoform (Fig. 1B).

ELISA (not shown) and Western blot (Fig. 1C) indicate that monospecific anti-PPARγ antisera were raised against both the MAP-14mer and MAP-19mer peptide-immunogens. A representative blot is shown for one anti-14mer rabbit (Rosita) and one anti-19mer rabbit (Patricia) compared to anti-PPARγ PoAb sc-7196 from Santa Cruz (Fig. 1C). Similar results were obtained for the second rabbit immunized with either MAP-14mer (Alice) or MAP-19mer (Penelope) peptide-immunogens and a second lot of sc-7196 (not shown). Serial 4–fold dilutions of rabbit IgG were tested for reactivity against synthetic peptides representing NH_2-terminal or C-terminal portions of the free peptides in antigen-down ELISAs to fine-point map the specificity of the PoAb anti-PPARγ produced against the MAP-14mer (Rosita, Fig. 2A) and the MAP-19mer (Patricia, Fig. 2B) immunogens. These results indicate that the intact peptide sequence is required for optimal reactivity of both anti-PPARγ peptide PoAbs.

3.3. Anti-PPARγ peptide monoclonal antibodies are pan-specific

Fusions were performed with sensitized spleens from two anti-MAP-14mer immunized mice (4MR and 5MP) and one anti-MAP-19mer immunized mouse (3MB). Four anti-14mer (2E2.F6, 3C11.E8.E1, 3F9.G8, and 4A5.H12) and two anti-19mer (6B4.A6 and 6D4.H4) hybridomas were selected for expansion and subcloning by limiting dilution. All six MoAbs were identified as μ-heavy (IgM) chain and κ light chain isotype antibodies. In addition to strong reactivity against rPPARγ1, ELISA (not shown) and Western blot (Fig. 3; only 6B4.A6 and 6D4.H4 are shown) data revealed that all six anti-PPARγ MoAbs crossreacted with rPPARα and rPPARβ/δ, indicating pan-PPAR isoform specificity. Blast protein sequence analysis revealed that the 19mer peptide contains longer stretches of unique structure; therefore, only anti-MAP-19mer MoAbs 6D4.H4 and 6B4.A6 were characterized further (Fig. 3). Whereas, 6D4.H4 reacted similarly with the four antigens tested (Fig. 3A), epitope mapping by ELISA demonstrated that 6B4.A6 reacted much stronger with both preparations of full-length rPPARγ1 and with the C-terminal 12 residues of the 19mer (C-term 19mer), rather than with the MAP-19mer peptide used as immunogen. MoAb 6B4.A6 reacted with 2–fold stronger relative intensity with rPPARγ1 than with rPPARα or PPARβ/δ by Western blot (Fig. 3B). In contrast, MoAb 6D4.H4 reacted more intensely with rPPARα than with rPPARβ/δ or rPPARγ1 (Fig. 3B). When the primary structure of the 12-residue peptide (DKIKFKHITPLQ) was compared to corresponding regions in PPARα and PPARβ/δ, the degree of sequence identity drops to 8.3% for both PPARα and PPARβ/δ and the similarity to 25% for PPARα and 33.3% for PPARβ/δ. Together, the results suggest that the epitope for 6B4.A6 maps to the C-terminus of the 19mer-peptide.

In addition, we compared our in-house produced MoAbs against a commercially available anti-PPARγ MoAb for specificity and reactivity. The product specification sheet for the anti-PPARγ MoAb sc-7273 from Santa Cruz states that it should crossreact with PPARα and PPARβ/δ. Therefore, we tested the reactivity of sc-7273 with rPPARα, PPARβ/δ and rPPARγ1 from Protein One by ELISA and Western immunodetection (Fig. 3C). Indeed, MoAb sc-7273 showed the strongest relative reactivity with rPPARβ/δ by ELISA, and crossreacted with the rPPARα and rPPARβ/δ as intensely as with rPPARγ1 by Western immunodetection, as well.

3.4. Bleeding diathesis and unusual pathology in response to anti-PPARγ antibodies

Because the rabbits and mice displayed unexpected pathologies over the course of the immunization schedule, necropsies were performed at the time of nonsurvival bleed-out. We observed significant gross pathology in both the rabbits and mice (Fig. 4). The PPARγ-specific peptides used as immunogens were coupled to inert carriers (by MAP technology), and therefore, the carrier alone would not be expected to elicit such a noteworthy response.

Mouse pathology—Upon sacrifice we observed significant abdominal fat with vascular hemorrhages and numerous adhesions around the intestines and spleens in mice immunized with either MAP-peptide-immunogen (Fig. 4A). Spleens from mice used for hybridoma fusions were encased in white fatty tissue with hemorrhagic vessels, were friable, and were decreased in mass compared to spleens from nonimmunized mice (Fig. 4A). For production of high titer antibody in ascites fluid, retired breeder mice were injected IP with 1×10^6 hybridoma cells producing the anti-PPARγ-14mer IgM isotype MoAb 4A5 and 3C11 or a well-characterized IgM isotype control MoAb, D73H, specific for the Bβ-chain of human fibrinogen (Rybarczyk et al., 2000). Ascites fluid recovered from the anti-14mer mice (4A5 and 3C11) was unusually bloody. Examination of the peritoneal cavity revealed that tumor cells were encased in highly vascularized, hemorrhagic white fatty tissue (Fig. 4B). Lymph nodes were hemorrhagic as well, consistent with increased vascular permeability (Fig. 4B). This degree of gross pathology was not observed in comparable ascites mice producing control IgM isotype MoAb, D73H (not shown). Epistaxis (nosebleeds) and bleeding into nail beds, hallmarks of a bleeding diathesis, were observed in mice used for the chronic thrombocytopenia study (Section 2.6) that were injected with purified IgG against platelets (positive control), anti-PPARγ-14mer or anti-PPARγ-19mer, but not in mice injected with control (nonimmune) IgG (Fig. 4C).

Rabbits—The immunized rabbits (n = 4) showed signs of cachexia, such as failure to gain weight at a normal rate and muscle wasting, which required supplementing the normal rabbit chow with fresh and dried fruit and alfalfa cubes to maintain weight. Early in the immunization protocol we observed signs of hypercoagulability suggestive of elevated plasma fibrinogen levels and a systemic acute phase response, necrotic skin lesions in the absence of fever, and signs of microthrombi in ear capillaries. After several months of booster injections, the rabbits acquired a bleeding diathesis as evidenced by prolonged bleeding following blood collection, lack of platelet plug formation during blood clotting for serum production, and unexplained purpura, although the rabbits were not anemic. Over the course of immunizations, collateral vessel growth was observed in the ears and healed skin lesions. None of these pathologies were observed in the mock-immunized rabbits.

The most remarkable gross pathology was noted in the ovaries from the immunized rabbits, which were enlarged 3– to 4–times normal size, likely due to edema from enhanced vascular permeability. Multiple enlarged, fluid filled antral and ruptured follicles with old blood clots indicative of excessive bleeding and necrosis were found in ovaries of immunized rabbits compared to ovaries from mock-immunized rabbits (Fig. 4D). Representative microscopic

fields of H&E stained ovarian tissue sections indicate that rabbits immunized with anti-PPARγ synthetic peptides contain significantly more follicles at later stages of maturation based on follicular cell proliferation (increased diameter and follicular cell stratification), antrum formation (fluid filled cavity) and the thecal cell zones surrounding growing follicles (Fig. 4E). The increased eosinophilic staining in the stromal compartment surrounding developing follicles in the PPARγ immunized rabbits denotes remarkable edema and bleeding, *i.e.*, eosinophilic fibrin(ogen) staining, compared to the mock-immunized rabbit.

3.5. Evidence of thrombocytopenia in rabbits producing anti-PPARγ antibodies

Analyses of rabbit blood chemistries performed on prebleed sera and bleed-5 sera were unremarkable. Complete blood counts, cell differentials and platelet counts were performed on appropriate samples taken at the same time as bleeds 3 and 5, only after observation of the aforementioned clinical anomalies. Whereas the cell differentials and platelet counts were in the normal range (290,000 to 650,000 platelets/μl) for rabbits immunized with the MAP-19mer (Penelope and Patricia), rabbits immunized with the MAP-14mer had low or borderline low normal platelet counts of 187,000/μl (Alice) and 290,000/μl (Rosita) after the third boost, which remained below normal (250,000/μl) in only one rabbit (Alice) at bleed-5; however, none of the rabbits were anemic. The mean platelet volume (MPV) was 3–fold higher in the rabbit with the lowest platelet counts (Alice), which is consistent with platelet activation and platelet destruction (immune thrombocytopenia) and new platelet production (Coban et al., 2008). Adherence of platelets on neutrophils and monocytes, known as satellitism, was observed (not shown), which is frequently associated with sporadic thrombocytopenia (Lazo-Langner et al., 2002).

3.6. Enhanced marrow megakaryocytopoiesis in rabbits producing anti-PPARγ antibodies

Enhanced maturation of bone marrow precursor cells into mature megakaryocytes (megakaryocytopoiesis) occurs in response to immune-mediated platelet destruction to restore circulating platelets to normal levels (Deutsch and Tomer, 2006). Quantification of the number of megakaryocytes per low power (10X) field indicated that enhanced megakaryocytopoiesis occurred in marrow of rabbits immunized with PPARγ synthetic peptides compared to control (mock-immunized) rabbits (Fig. 5A). Representative H&E stained sections of bone marrow from a control rabbit (Magnolia, Fig. 5B) and the anti-PPARγ 14mer rabbit (Alice, Fig. 5C and 5D) are shown. Emperipolesis, the engulfment of whole cells by megakaryocytes, occurs frequently in thrombocytopenia (Muhury et al., 2009). The presence of neutrophils and lymphocytes in the cytoplasm of megakaryocytes was frequently noted in the rabbits immunized with the PPARγ synthetic peptides, especially in the rabbit with sustained thrombocytopenia (Alice, Fig. 5D).

3.7. Thrombocytopenia in PPARγ MoAb ascites mice and induction of megakaryocytopoiesis in spleens of mice passively administered anti-PPARγ PoAbs

Because we observed thrombocytopenia in the anti-PPARγ-14mer rabbits, platelet counts were performed on ascites mice producing MoAb 3C11 (anti-PPARγ-14mer; IgM isotype) and, as an isotype control, D73H (anti-Bβ-chain of human fibrinogen) (Rybarczyk et al., 2000). MoAb D73H was used as a control hybridoma line for ascites production for two reasons. First, MoAb D73H produces an IgM, κ light chain isotype antibody, as does the anti-PPARγ-14mer 3C11. Second, fibrinogen is a platelet α-granule constituent that it is not exposed on the surface of platelets unless they are activated and, thus, should be unavailable for binding to D73H. Ascites production of anti-PPARγ 3C11 lowered platelet counts in Balb/c mice by 43.5% compared to an 8% reduction in response to side-by-side production of the control IgM isotype MoAb, D73H, suggesting immune-mediated destruction of circulating platelets only in the anti-PPARγ producing ascites mice (Fig. 6A). To determine whether anti-PPARγ 14mer and 19mer PoAbs were able to induce thrombocytopenia, we

compared platelet counts in naïve Balb/c mice subjected to acute (one injection) or chronic (4 injections over 9 days) experimental thrombocytopenia. Although reduction in platelet counts reached statistical significance for positive controls of both the acute and chronic models of experimental thrombocytopenia, neither anti-PPARγ PoAbs reduced platelet counts in naïve Balb/c mice (Fig. 6B and 6C).

Because a failure to induce thrombocytopenia could be due to compensatory megakaryocytopoiesis and new platelet production, we quantified the number of megakaryocytes per low power field (20X) in spleens from mice subjected to chronic administration of anti-PPARγ 14mer or 19mer IgG. The spleen is a predominant site for enhanced megakaryocytopoiesis in mice. The results indicate that a 4–8–fold increase in megakaryocyte production occurred in response to four injections of anti-PPARγ 14-mer or 19-mer IgG over 9 days. Chronic administration of the positive control anti-platelet IgG promoted a >10–fold increase in megakaryocyte production (Fig. 7A). Representative H&E stained sections of spleen from nonimmune control (Fig. 7B), anti-platelet (Fig. 7C), and anti-PPARγ-19mer (Fig. 7D) IgG-treated mice demonstrate enhanced megakaryocytopoiesis in spleens.

4. Discussion

To further our studies on the functional significance of platelet-derived PPARγ, we needed antibodies that could detect PPARγ in blood and blood cells. In previous studies, we used the Biomol and Calbiochem anti-PPARγ PoAbs (Feldon et al., 2006, Ray et al., 2008, O'Brien et al., 2008); however, per product specification sheets, neither of these PoAbs could be used to detect PPARγ in the presence of serum albumin. Also, for unknown reasons during the course of these studies, the Biomol and Calbiochem PoAbs became no longer available, prompting us to produce our own anti-PPARγ rabbit PoAbs and MoAbs. Unexpectedly, during the course of production and characterization of PoAbs and MoAbs against PPARγ peptide immunogens, our work produced two key findings. First, we observed significant and unusual pathology in the immunized rabbits and mice over the time course of immunization. Second, although the PoAbs produced were monospecific for PPARγ, the MoAbs produced against the same 14mer and 19mer peptide-immunogens crossreacted with PPARα and PPARβ/δ.

The remarkable pathology we observed in both rabbits and mice suggested that production of anti-PPARγ antibodies produced an immune complex disease similar to immune thrombocytopenia. In particular, we observed low platelet counts in rabbits immunized with the PPARγ 14mer peptide-immunogen. In addition, signs of increased vascular permeability were observed in all four immunized rabbits including unexplained purpura, enlarged ovaries likely due to edema, plasma leakage and excessive bleeding from ruptured and necrotic ovarian follicles. Excessive hemorrhaging was observed in the spleens of immunized mice and in the lymph nodes and intraperitoneal tumors of the mice injected with anti-PPARγ hybridoma cells for MoAb production in ascites fluid. Furthermore, platelet counts were substantially reduced in the anti-PPARγ-14mer 3C11 (IgM isotype) ascites mice, but not in the D73H ascites mice producing an IgM isotype MoAb against the Bβ-chain of human fibrinogen (Rybarczyk et al., 2000). Platelet depletion and increased MPV reflect the state of thrombogenesis (Hekimsoy et al., 2004). High MPV is associated with low platelet counts due to platelet destruction (immune thrombocytopenia) and platelet activation (Coban et al., 2008, Sullivan et al., 1995). Increase in MPV occurs in patients with metabolic syndrome, stroke and diabetes mellitus (Zuberi et al., 2008), contributing to the increased vascular complications and endothelial cell dysfunction observed (Hekimsoy et al., 2004). Although we observed increased MPV in only one rabbit with low platelet counts, platelet functions were clearly compromised in all four rabbits and 3C11 ascites

mice. Together, these results support the hypothesis that immune-mediated destruction of platelets occurred in animals immunized with the PPARγ peptide-immunogens due to crossreactivity of the elicited anti-PPARγ antibodies with platelet-derived PPARγ.

The mechanisms by which anti-PPARγ antibodies induce sporadic or transient thrombocytopenia are presently unknown. However, immune-mediated destruction of platelets occurs during idiopathic/immune thrombocytopenia purpura, which is frequently caused by IgG isotype antibodies against platelet membrane glycoprotein complexes αIIb-IIIa or Ib-IX (Hou et al., 1995). Furthermore, antibodies against GP1bα are frequently used to induce thrombocytopenia in mice. Acute thrombocytopenia occurs within 60 min after injecting mice with purified rat PoAb IgG raised against platelet GP1bα (R300) and, according to the R300 product specification sheet, mouse platelet counts can be reduced up to 95% using 4 μg/g body weight and remain low for 48 to 72 hours. Therefore, we determined whether passive administration of purified anti-PPARγ-14mer or anti-PPARγ-19mer IgG could reduce platelet counts in naïve mice using both acute and chronic models of experimental immune-mediated thrombocytopenia. Neither anti-PPARγ-14mer nor anti-PPARγ-19mer IgG induced thrombocytopenia in the acute or chronic model of immune-mediated platelet destruction. However, megakaryocytopoiesis was enhanced 4–8–fold in mouse spleens of mice treated with anti-PPARγ-14mer or anti-PPARγ-19mer IgG suggesting that compensatory platelet production maintained normal levels of blood platelets. Enhanced production of megakaryocytes in the bone marrow of all four rabbits immunized with PPARγ synthetic peptides was also observed. Compensatory platelet production due to enhanced megakaryocytopoiesis would explain the thrombocytopenia and bleeding anomalies observed in both rabbits and mice immunized with PPARγ peptide-immunogens. These data further support the hypothesis that immune-mediated destruction of platelets occurred in animals immunized with the PPARγ peptide-immunogens due to crossreactivity of the elicited anti-PPARγ antibodies with platelet-derived PPARγ.

The advent of MoAb production to design an antibody that exquisitely recognizes a defined epitope of a given molecule using the method developed by Kohler and Milstein in 1975 (Kohler and Milstein, 1975) has revolutionized basic biomedical research, diagnostics and disease treatment. MoAbs produce only one specific antibody isotype against a defined epitope; however, there is no guarantee that this antibody is monospecific against the native antigen. Although the PoAbs we produced against the PPARγ-14mer and PPARγ-19mer peptide-immunogens were monospecific for rPPARγ, the MoAbs we produced against the same peptide-immunogens crossreacted with rPPARα and rPPARβ/δ in addition to rPPARγ. Indeed, two commercially available anti-PPARγ antibodies from Santa Cruz Biotechnology show strikingly similar results as reported herein. PoAb anti-PPARγ sc-7196 is monospecific for rPPARγ while MoAb anti-PPARγ sc-7273 crossreacts with rPPARα, rPPARβ/δ and rPPARγ. The peptide immunogen used to produce sc-7273 maps to the last 25 amino acids of PPARγ, an epitope structurally distinct from the 14mer and 19mer used in this study, suggesting that selection of the immunodominant hybridomas producing these anti-PPARγ MoAbs responded to a peptide conformation and primary structure shared by PPARα, PPARβ/δ and PPARγ. The lack of monospecificity of the anti-PPARγ MoAbs described in this report and available commercially (sc-7273) is a striking example of one of the major pitfalls associated with production of MoAbs against closely related molecules—monoclonicity does not guarantee monospecificity. Santa Cruz anti-PPARγ MoAb, sc-7273, is frequently reported in the literature for immunodetection of PPARγ. Currently, 132 citations using this antibody are listed on the Santa Cruz web page (http://www.scbt.com/datasheet-7273-ppargamma-e-8-antibody.html). In that the apparent molecular weights of the three PPAR isoforms fall within 49–54 kDa, it is important that the specificities of antibodies used for detection are thoroughly vetted.

Amino acid stretches as small as 4–6 residues define highly immunogenic determinants (Hopp and Woods, 1981), and the potential for representation of such determinants in unrelated molecules is high. The ability to produce highly specific MoAbs against peptide-immunogens is further complicated when the target of interest is a member of a closely related gene family such as the PPARs. The hybridoma cell line selected for a specific MoAb produces the antibody reactivity of one plasma cell that responded to the presentation of a single peptide-immunogen conformation in solution selected from an undetermined number of peptide-immunogen conformations presented to the immune system during production of PoAbs. Small peptide sequences inherently lack defined secondary and tertiary structure. Thus, the number of conformations that synthetic peptides adopt and the length of time such a conformation is maintained is unknown. Indeed, development of anti-peptide vaccines to prevent HIV infection has been hindered by the lack of structure in aqueous solution of the major neutralizing determinant on envelope protein gp120 of HIV-1 (Chandrasekhar et al., 1991). Our strategy for selection of primary structure for choice of peptide immunogens takes advantage of known parameters that restrict random structure (Section 2.2). However, our strategy is not foolproof even though we successfully produced a number of anti-peptide MoAbs against closely related molecules (Simpson-Haidaris et al., 1989a, Simpson-Haidaris et al., 1989b, Fay et al., 1991, Odrljin et al., 1996, Meh et al., 2001).

Others have shown the lack of monospecificity of MoAbs as well. For example, a MoAb that binds preferentially to integrin αIIbβ3 on activated platelets (7E3) crossreacts with integrin CD11b/CD18 (Mac-1) on activated monocytes (Simon et al., 1997, Schwarz et al., 2002). MoAb 7E3, the parent antibody of abciximab (ReoPro), is used to prevent platelet aggregation in patients undergoing angioplasty (EPIC-Investigation, 1994). It is thought that inhibition of CD11b/CD18-dependent adhesion and αIIb/β3-dependent function may jointly contribute to the regulation of vascular repair and sustained clinical benefits observed with abciximab after angioplasty (Simon et al., 1997). In this example, crossreactivity of MoAb 7E3 with integrin CD11b/CD18 on monocytes appears to have a beneficial clinical effect; however, such a positive result may not always hold true. Additionally, there are the seven publications regarding the lack of specificity of multiple antibodies from commercial and academic sources that are used for mapping receptors of therapeutic interest, including antibodies specific for adrenergic, muscarinic, and dopaminergic receptors (Kirkpatrick, 2009). Because it is important to properly identify the appropriate PPAR isoform in various tissues, clarity in the reactivity of MoAbs and PoAbs against the PPAR isoforms (α, β/δ and γ), which exhibit highly conserved primary structure, functional domains and nearly identical apparent molecular weights, is essential.

PPARγ agonists, including the thiazolidinediones, exert beneficial effects on glycemic control and reduction of inflammatory cardiovascular risk factors, making them attractive agents for treatment of type 2 diabetics at high risk for cardiovascular disease (Spinelli et al., 2008). PPARs exert anti-inflammatory effects by inhibiting the induction of pro-inflammatory cytokines, adhesion molecules and extracellular matrix proteins or by stimulating the production of anti-inflammatory molecules (Kostadinova et al., 2005). Moreover, PPARγ agonists inhibit platelet aggregation and release of storage granule constituents such as CD40 ligand and thromboxane A_2 (Akbiyik et al., 2004), potent mediators of inflammation and cardiovascular disease. Systemic inflammation is clearly linked with adverse prognosis in patients with cancer as well (Sahni et al., 2009). Release of platelet granule constituents plays a critical role in maintaining the integrity of tumor vasculature to prevent hemorrhaging, and neither platelet aggregation nor thrombi formation is required for this function (Ho-Tin-Noe et al., 2008, Ho-Tin-Noe et al., 2009). It is intriguing to speculate that release of platelet-derived PPARγ and uptake by vascular endothelium, perhaps from microparticles, plays a role in maintaining the integrity of tumor

vasculature to prevent bleeding. In that PPARγ ligands promote apoptosis, induce cell-cycle arrest, promote cell differentiation and inhibit tumor angiogenesis and metastasis, PPARγ is considered a potential therapeutic target in hematological malignancies (Garcia-Bates et al., 2008a, Garcia-Bates et al., 2008b) and cancers of epithelial origin (Panigrahy et al., 2005, Tachibana et al., 2008, Murphy and Holder, 2000). Furthermore, PPARγ ligands decrease vascular permeability and leukostasis associated with diabetic retinopathy (Yanagi, 2008), suggesting that PPARγ plays a global role in maintenance of vascular homeostasis.

In summary, the observations reported herein support the assertion that the validity of MoAbs and PoAbs produced by academic investigators and commercial vendors for biomedical research and ultimately clinical therapy cannot be taken at face value. A thorough vetting of the specificity of such reagents is required to allow accurate interpretation of experimental data or clinical trial outcomes proving the identity or efficacy of putative drug targets.

Acknowledgments

The authors would like to thank Michael Anne and Tse-Yao Wang for technical assistance and Randall Rossi for assistance with the Heska Hematology Analyzer. This work was supported by non-federal funds (RPP). PJS-H would like to dedicate this work to the memory and spirit of her mother, Agnes Day Simpson, who passed away at the age of 94 on December 16, 2009.

Abbreviations

CFA	Complete Freund's Adjuvant
H&E	hematoxylin and eosin
IFA	Incomplete Freund's Adjuvant
MBP	maltose binding protein
MPV	mean platelet volume
MK	megakaryocytes
MAP	Multiple Antigen Peptide
MoAb(s)	monoclonal antibody(ies)
NRS	normal rabbit serum
PPAR(s)	peroxisome proliferator-activated receptor(s)
PT	platelets
PoAb(s)	polyclonal antibody(ies)
rPPAR	recombinant PPAR
RXR	retinoid-X-receptor

References

Akbiyik F, Ray DM, Gettings KF, Blumberg N, Francis CW, Phipps RP. Human bone marrow megakaryocytes and platelets express PPARgamma, and PPARgamma agonists blunt platelet release of CD40 ligand and thromboxanes. Blood 2004;104:1361–1368. [PubMed: 15130939]

Ali FY, Davidson SJ, Moraes LA, Traves SL, Paul-Clark M, Bishop-Bailey D, Warner TD, Mitchell JA. Role of nuclear receptor signaling in platelets: antithrombotic effects of PPARbeta. Faseb J 2006;20:326–328. [PubMed: 16368717]

Altschul SF, Madden TL, Schaffer AA, Zhang J, Zhang Z, Miller W, Lipman DJ. Gapped BLAST and PSI-BLAST: a new generation of protein database search programs. Nucleic Acids Res 1997;25:3389–3402. [PubMed: 9254694]

Andrew, SM.; Titus, JA. Purification of immunoglobulin G.. Curr. Protoc. Immunol. 2001. Chapter 2, Unit 2 7

Chandrasekhar K, Profy AT, Dyson HJ. Solution conformational preferences of immunogenic peptides derived from the principal neutralizing determinant of the HIV-1 envelope glycoprotein gp120. Biochemistry 1991;30:9187–9194. [PubMed: 1892828]

Coban E, Adanir H, Bilgin D. The association of mean platelet volume levels with hypertensive retinopathy. Platelets 2008;19:115–118. [PubMed: 17852776]

Courtney MA, Stoler MH, Marder VJ, Simpson-Haidaris PJ. Developmental expression of mRNAs encoding platelet proteins in rat megakaryocytes. Blood 1991;77:560–568. [PubMed: 1991167]

Deutsch VR, Tomer A. Megakaryocyte development and platelet production. Br J Haematol 2006;134:453–466. [PubMed: 16856888]

Epic-Investigation. Use of a monoclonal antibody directed against the platelet glycoprotein IIb/IIIa receptor in high-risk coronary angioplasty. The EPIC Investigation. N Engl J Med 1994;330:956–961. [PubMed: 8121459]

Fay PJ, Haidaris PJ, Smudzin TM. Human factor VIIIa subunit structure. Reconstruction of factor VIIIa from the isolated A1/A3-C1-C2 dimer and A2 subunit. J. Biol. Chem 1991;266:8957–8962. [PubMed: 1902833]

Feldon SE, O'loughlin C W, Ray DM, Landskroner-Eiger S, Seweryniak KE, Phipps RP. Activated human T lymphocytes express cyclooxygenase-2 and produce proadipogenic prostaglandins that drive human orbital fibroblast differentiation to adipocytes. Am J Pathol 2006;169:1183–1193. [PubMed: 17003477]

Garcia-Bates TM, Bernstein SH, Phipps RP. Peroxisome proliferator-activated receptor gamma overexpression suppresses growth and induces apoptosis in human multiple myeloma cells. Clin Cancer Res 2008a;14:6414–6425. [PubMed: 18927280]

Garcia-Bates TM, Lehmann GM, Simpson-Haidaris PJ, Bernstein SH, Sime PJ, Phipps RP. Role of peroxisome proliferator-activated receptor gamma and its ligands in the treatment of hematological malignancies. PPAR Res 2008b;2008:834612. [PubMed: 18528522]

Gervois P, Torra IP, Chinetti G, Grotzinger T, Dubois G, Fruchart JC, Fruchart-Najib J, Leitersdorf E, Staels B. A truncated human peroxisome proliferator-activated receptor alpha splice variant with dominant negative activity. Mol Endocrinol 1999;13:1535–1549. [PubMed: 10478844]

Hekimsoy Z, Payzin B, Ornek T, Kandogan G. Mean platelet volume in Type 2 diabetic patients. J. Diabetes Complications 2004;18:173–176. [PubMed: 15145330]

Ho-Tin-Noe B, Goerge T, Cifuni SM, Duerschmied D, Wagner DD. Platelet granule secretion continuously prevents intratumor hemorrhage. Cancer Res 2008;68:6851–6858. [PubMed: 18701510]

Ho-Tin-Noe B, Goerge T, Wagner DD. Platelets: guardians of tumor vasculature. Cancer Res 2009;69:5623–5626. [PubMed: 19584268]

Hopp TP, Woods KR. Prediction of protein antigenic determinants from amino acid sequences. Proc Natl Acad Sci U S A 1981;78:3824–3828. [PubMed: 6167991]

Hou M, Stockelberg D, Kutti J, Wadenvik H. Antibodies against platelet GPIb/IX, GPIIb/IIIa, and other platelet antigens in chronic idiopathic thrombocytopenic purpura. Eur J Haematol 1995;55:307–314. [PubMed: 7493677]

Kirkpatrick P. Specificity concerns with antibodies for receptor mapping. Nat Rev Drug Discov 2009;8:278. [PubMed: 19348032]

Kohler G, Milstein C. Continuous cultures of fused cells secreting antibody of predefined specificity. Nature 1975;256:495–497. [PubMed: 1172191]

Kostadinova R, Wahli W, Michalik L. PPARs in diseases: control mechanisms of inflammation. Curr. Med. Chem 2005;12:2995–3009. [PubMed: 16378501]

Larsen LK, Amri EZ, Mandrup S, Pacot C, Kristiansen K. Genomic organization of the mouse peroxisome proliferator-activated receptor beta/delta gene: alternative promoter usage and splicing

yield transcripts exhibiting differential translational efficiency. Biochem J 2002;366:767–775. [PubMed: 12059785]

Lazo-Langner A, Piedras J, Romero-Lagarza P, Lome-Maldonado C, Sanchez-Guerrero J, Lopez-Karpovitch X. Platelet satellitism, spurious neutropenia, and cutaneous vasculitis: casual or causal association? Am J Hematol 2002;70:246–249. [PubMed: 12111772]

Liu F, Morris S, Epps J, Carroll R. Demonstration of an activation regulated NF-kappaB/I-kappaBalpha complex in human platelets. Thromb Res 2002;106:199–203. [PubMed: 12297126]

Meh DA, Mosesson MW, Siebenlist KR, Simpson-Haidaris PJ, Brennan SO, Diorio JP, Thompson K, Di Minno G. Fibrinogen Naples I (Bβ A68T) nonsubstrate thrombin-binding capacities. Thromb Res 2001;103:63–73. [PubMed: 11434947]

Michalik L, Auwerx J, Berger JP, Chatterjee VK, Glass CK, Gonzalez FJ, Grimaldi PA, Kadowaki T, Lazar MA, O'rahilly S, Palmer CN, Plutzky J, Reddy JK, Spiegelman BM, Staels B, Wahli W. International Union of Pharmacology. LXI. Peroxisome proliferator-activated receptors. Pharmacol. Rev 2006;58:726–741. [PubMed: 17132851]

Moraes LA, Paul-Clark MJ, Rickman A, Flower RJ, Goulding NJ, Perretti M. Ligand-specific glucocorticoid receptor activation in human platelets. Blood 2005;106:4167–4175. [PubMed: 16131566]

Moraes LA, Swales KE, Wray JA, Damazo A, Gibbins JM, Warner TD, Bishop-Bailey D. Nongenomic signaling of the retinoid X receptor through binding and inhibiting Gq in human platelets. Blood 2007;109:3741–3744. [PubMed: 17213293]

Muhury M, Mathai AM, Rai S, Naik R, Pai MR, Sinha R. Megakaryocytic alterations in thrombocytopenia: a bone marrow aspiration study. Indian J. Pathol. Microbiol 2009;52:490–494. [PubMed: 19805953]

Murphy GJ, Holder JC. PPAR-gamma agonists: therapeutic role in diabetes, inflammation and cancer. Trends Pharmacol. Sci 2000;21:469–474. [PubMed: 11121836]

O'brien JJ, Spinelli SL, Tober J, Blumberg N, Francis CW, Taubman MB, Palis J, Seweryniak KE, Gertz JM, Phipps RP. 15-deoxy-{Delta}12,14-PGJ2 enhances platelet production from megakaryocytes. Blood 2008;112:4051–4060. [PubMed: 18755987]

Odrljin TM, Rybarczyk BJ, Francis CW, Lawrence SO, Hamaguchi M, Simpson-Haidaris PJ. Calcium modulates plasmin cleavage of the fibrinogen D fragment © chain N-terminus: mapping of monoclonal antibody J88B to a plasmin sensitive domain of the © chain. Biochim. Biophys. Acta 1996;1298:69–77. [PubMed: 8948490]

Panigrahy D, Huang S, Kieran MW, Kaipainen A. PPARgamma as a therapeutic target for tumor angiogenesis and metastasis. Cancer Biol Ther 2005;4:687–693. [PubMed: 16082179]

Ray DM, Spinelli SL, O'brien JJ, Blumberg N, Phipps RP. Platelets as a novel target for PPARgamma ligands: implications for inflammation, diabetes, and cardiovascular disease. BioDrugs 2006;20:231–241. [PubMed: 16831022]

Ray DM, Spinelli SL, Pollock SJ, Murant TI, O'brien JJ, Blumberg N, Francis CW, Taubman MB, Phipps RP. Peroxisome proliferator-activated receptor gamma and retinoid X receptor transcription factors are released from activated human platelets and shed in microparticles. Thromb. Haemost 2008;99:86–95. [PubMed: 18217139]

Rybarczyk BJ, Pereira M, Simpson-Haidaris PJ. Characterization of a monoclonal antibody, D73H, that maps to a highly conserved region on fibrinogen Bβ chain. Thromb. Haemost 2000;84:43–48. [PubMed: 10928468]

Sahni A, Arevalo MT, Sahni SK, Simpson-Haidaris PJ. The VE-cadherin binding domain of fibrinogen induces endothelial barrier permeability and enhances transendothelial migration of malignant breast epithelial cells. Int J Cancer 2009;125:577–584. [PubMed: 19358279]

Schwarz M, Nordt T, Bode C, Peter K. The GP IIb/IIIa inhibitor abciximab (c7E3) inhibits the binding of various ligands to the leukocyte integrin Mac-1 (CD11b/CD18, alpha(M)beta(2)). Thromb Res 2002;107:121–128. [PubMed: 12431477]

Simon DI, Xu H, Ortlepp S, Rogers C, Rao NK. 7E3 monoclonal antibody directed against the platelet glycoprotein IIb/IIIa cross-reacts with the leukocyte integrin Mac-1 and blocks adhesion to fibrinogen and ICAM-1. Arteriosclerosis, Thrombosis & Vascular Biology 1997;17:528–535.

Simpson-Haidaris PJ, Francis CW, Sporn LA, Arvan DS, Collichio FA, Marder VJ. Megakaryocyte and hepatocyte origins of human fibrinogen biosynthesis exhibit hepatocyte-specific expression of gamma chain-variant polypeptides. Blood 1989a;74:743–750.

Simpson-Haidaris PJ, Peerschke EI, Marder VJ, Francis CW. The C-terminal sequences of the γ57.5 chain of human fibrinogen constitute a plasmin sensitive epitope that is exposed in crosslinked fibrin. Blood 1989b;74:2437–2444.

Spinelli SL, Casey AE, Pollock SJ, Gertz JM, Mcmillan DH, Narasipura SD, Mody NA, King MR, Maggirwar SB, Francis CW, Taubman MB, Blumberg N, Phipps RP. Platelets and megakaryocytes contain functional nuclear factor-kappaB. Arterioscler Thromb Vasc Biol 2010;30:591–598. [PubMed: 20042710]

Spinelli SL, O'brien JJ, Bancos S, Lehmann GM, Springer DL, Blumberg N, Francis CW, Taubman MB, Phipps RP. The PPAR-platelet connection: Modulators of inflammation and potential cardiovascular effects. PPAR Res 2008;2008:328172. [PubMed: 18288284]

Sullivan PS, Manning KL, Mcdonald TP. Association of mean platelet volume and bone marrow megakaryocytopoiesis in thrombocytopenic dogs: 60 cases (1984-1993). J. Am. Vet. Med. Assoc 1995;206:332–334. [PubMed: 7751241]

Tachibana K, Yamasaki D, Ishimoto K, Doi T. The role of PPARs in cancer. PPAR Res 2008;2008:102737. [PubMed: 18584037]

Tontonoz P, Spiegelman BM. Fat and beyond: the diverse biology of PPARgamma. Annu. Rev. Biochem 2008;77:289–312. [PubMed: 18518822]

Vassilev AO, Lorenz DR, Tibbles HE, Uckun FM. Role of the leukemia-associated transcription factor STAT3 in platelet physiology. Leuk. Lymphoma 2002;43:1461–1467. [PubMed: 12389630]

Yanagi Y. Role of peoxisome proliferator activator receptor gamma on blood retinal barrier breakdown. PPAR Res 2008;2008:679237. [PubMed: 18309374]

Zuberi BF, Akhtar N, Afsar S. Comparison of mean platelet volume in patients with diabetes mellitus, impaired fasting glucose and non-diabetic subjects. Singapore Med. J 2008;49:114–116. [PubMed: 18301837]

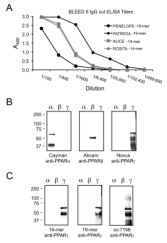

Figure 1. Bleed-out ELISA titers and Western immunodetection of rPPAR isoforms

The relative titer of each rabbit antiserum was determined against its respective immunogen by antigen-down ELISA. Four–fold dilutions of serum starting at 1:100 were tested in duplicate for each rabbit. A representative titration curve is shown (*panel A*). Recombinant human PPARα, β and γ1 were loaded at 1 μg/lane for Western immunodetection using commercially purchased rabbit anti-PPARα and anti-PPARβ and chicken anti-PPARγ (*panel B*). Ammonium sulfate IgG fractions of rabbit anti-PPARγ antisera were diluted 1:1000 for Western immunodetection. A representative blot is shown for one anti-14mer (Rosita) and one anti-19mer (Patricia) compared to a commercially available rabbit anti-PPARγ antibody, sc-7196 (*panel C*).

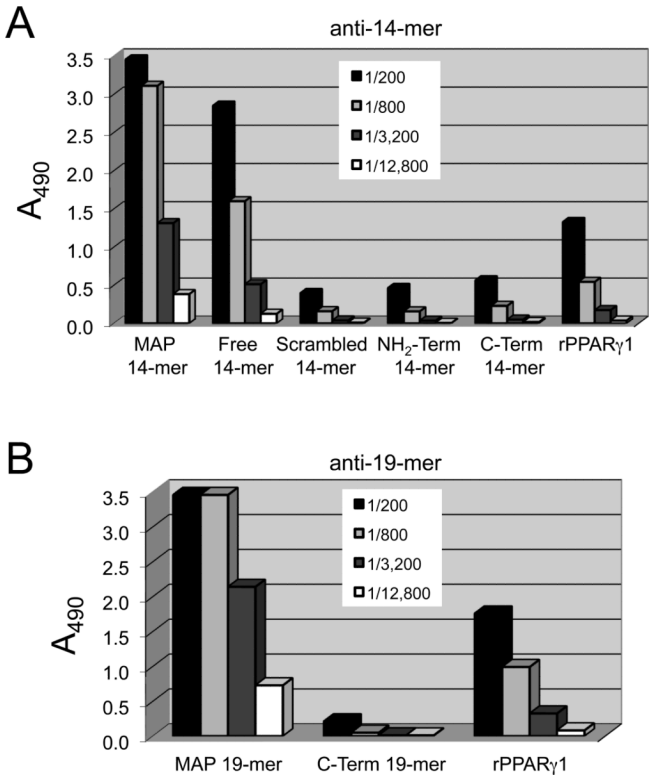

Figure 2. Epitope mapping of PoAb anti-PPARγ peptide IgG

Various peptides corresponding to the truncated portions of the peptide-immunogens were used in antigen-down ELISA to fine-point map the epitope reactivity of the PoAbs. A representative titration by ELISA is shown for one anti-14mer peptide rabbit (Rosita) in *panel A* and one anti-19mer rabbit (Patricia) in *panel B.*

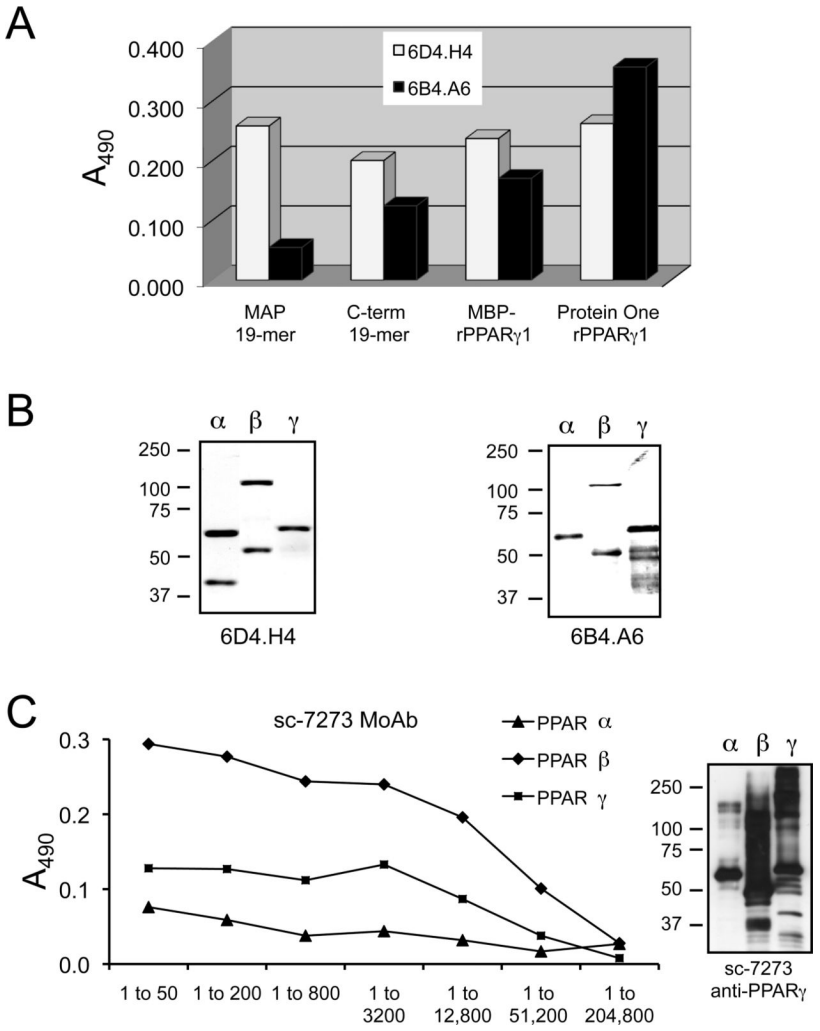

Figure 3. Crossreactivity determination of anti-PPARγ MoAbs

Conditioned media from two anti-19mer MoAbs, 6D4.H4 and 6B4.H4, were tested by ELISA for relative specificity for the following antigens: the original peptide-immunogen (MAP-19mer), a synthetic peptide corresponding to the C-terminal 12 residues of the original 19mer, rPPARγ1 isolated from *E. coli* as a fusion protein with MBP (MBP-rPPARγ1), and purified rPPARγ1 from Protein One (*panel A*). The crossreactivity of the two anti-19mer PPARγ peptide MoAbs against rPPARα and PPARβ was determined by Western immunodetection (*panel B*). An anti-PPARγ MoAb from Santa Cruz Biotechnology (sc-7273) was tested for specificity against rPPARα, PPARβ and PPARγ1 by ELISA (*panel C, left*) and Western (*panel C, right)* immunodetection.

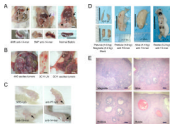

Figure 4. Unusual organ pathology is associated with mice and rabbits immunized with PPARγ synthetic peptides

The upper panels (*left to right panel A*) show abdominal organs *in situ* of two Balb/c mice immunized with PPARγ MAP-14mer synthetic peptide-immunogen and one normal mouse; the *lower panel A* pictures show the gross pathology of the sensitized or normal spleen from each mouse shown in *upper panel A*. The thin arrows (*upper left and middle panel A*) point to the adhesions of abdominal fat/connective tissue around the intestines, liver, and spleen in the immunized mice (4MR and 5MP); the asterisks denote hemorrhagic blood vessels; in the normal mouse, the abdominal fat presents as a visceral deposit in the lower abdomen as denoted by the thick arrowhead (*upper right panel A*). The thick arrow indicates the tip of the spleen in each mouse. The spleens from the immunized mice (*lower left and middle panel A*) were encased in fatty tissue, which was not present around the spleen from a normal mouse. Furthermore, the spleens from the 5MP anti-14mer mouse (*lower middle panel A*) and 3MB anti-19mer mouse (*not shown*) were friable and hemorrhagic, which we have not observed in the sensitized spleens from other mice used by us for hybridoma production over the past 23 years. The black bars in *upper right panel A* represent 0.25 inches and in *lower right panel A*, 0.5 inches. The tumors in the peritoneal cavities of the ascites mice were encased in highly vascularized, hemorrhagic white fatty tissue (*left and right panel B*) and the lymph nodes (LN) were hemorrhagic (*middle panel B*). The white bars (*left and right panel B*) represent 0.25 inches and the black bar (*middle panel B*) represents 0.5 inches. A bleeding tendency, indicative of abnormal primary hemostasis (*i.e.*, disrupted platelet aggregation), was observed in the toenail beds (arrows) of mice injected with purified rabbit IgG raised against rat platelets (*panel C*, anti-PT IgG) and IgG raised against human PPARγ synthetic peptides (*panel C*, anti-14mer and anti-19mer), but not in the toenail beds of mice treated with nonimmune rabbit IgG (*panel C*, NRS-IgG). The most striking pathology observed in the immunized rabbits was enlarged ovaries (Patricia, Alice and Rosita), which contained numerous necrotic and unruptured follicles compared to the ovaries from the mock-immunized rabbits (Petunia and Magnolia) (*panel D*). The black bars in each picture of *panel D* represent 1 inch and the length and weight of each ovary is indicated. Histomorphological examination of the ovaries (*panel E*) from mock-immunized (Magnolia) and rabbits immunized with PPARγ MAP-14mer (Alice and Rosita) or MAP-19mer (Patricia) peptide-immunogens confirmed the enhanced bleeding tendency observed in the immunized rabbits as denoted by increased eosinophilic staining of the tissue parenchyma indicating the presence of fibrinogen and/or fibrin, and by the old blood clots remaining in the enlarged follicles.

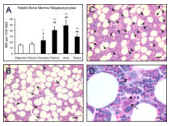

Figure 5. Enhanced megakaryocytopoiesis occurs in rabbit bone marrow in response to immunization with human PPARγ-synthetic peptides

The number of megakaryocytes (MK) per 10X brightfield was quantified as described in *Section 2.5*. Statistical analysis was performed by paired Students t-test to compare control rabbits (Magnolia, */**) and (Petunia, #/##) to immunized rabbits with p-values as follows: (*) $p = 0.0012$; (#) $p = 0.0160$; (**) $p < 0.0001$; and (##) $p < 0.0001$. Representative H&E stained bone marrow sections are shown for a mock-immunized rabbit (*panel B*, Magnolia) and the rabbit showing sustained low platelet counts over the course of the immunization schedule (*panels C and D*, Alice). The bars in *panels B and C* represent 50 μm of images taken with the 20X objective; the bar in *panel D* represents 10 μm of images taken with the 100X objective. The arrows in *panels B and C* denote megakaryocytes; the asterisks in *panel C* denote probable megakaryocytes sectioned through portions of the cytoplasm only—these were not included in the quantitation. In *panel D*, the arrows point to neutrophils and the arrowhead points to lymphocytes engulfed by megakaryocytes (emperipolesis).

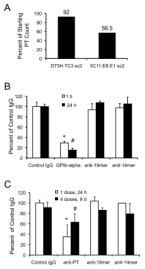

Figure 6. Mouse models of acute and chronic immune-mediated thrombocytopenia

Changes in platelet counts due to antibody treatment are presented as a percentage of the mean platelet ± SD of control (IgG) platelet counts at each time point. Relative platelet counts were reduced in response to high titer MoAb production of anti-PPARγ-14mer 3C11.E8.E1 but not in response to anti-human fibrinogen Bβ-chain D73H.7C3 in ascites mice (*panel A)* (sc2, subclone 2). Rat anti-GP1bα IgG induced acute thrombocytopenia (*p = 0.0134) in 1 hr that was sustained for 24 hr (#p = 0.0029) (*panel B*). No differences in platelet counts were observed in mice treated with either anti-19mer or anti-14mer IgG (*panel B*). Anti-platelet IgG induced significant thrombocytopenia 24 hr after the first injection (*p = 0.0111) that was sustained over nine days with injections of anti-platelet IgG repeated every 72 hr (#p = 0.0234) (*panel C*). Chronic administration of anti-PPARγ-19-mer or anti-PPARγ-14mer did not induce thrombocytopenia in naïve mice (*panel C*).

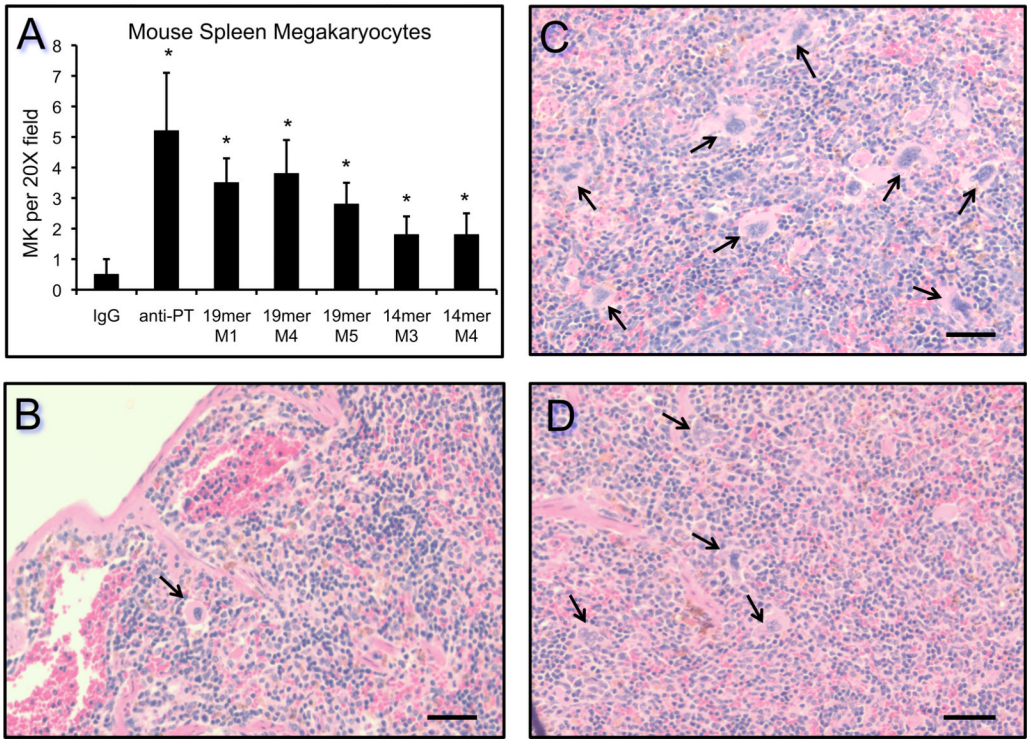

Figure 7. Passive administration of rabbit anti-platelet IgG and anti-PPARγ IgG induces megakaryocytopoiesis in mouse spleen

The data is presented graphically (*panel A*) as the average number of megakaryocytes per 20X field (n=13 per condition), the positive control (*anti-PT*), the negative control (*IgG*), mice injected with anti-PPARγ-19mer (*19mer, M1, M4, M5*), and mice injected with anti-PPARγ-14mer (*14mer, M3, M4*). Statistical significance (*$p < 0.0001$) was achieved in all conditions compared to control IgG (*panel A*). Representative H&E stained spleen sections are shown for a negative control mouse injected with nonimmune IgG (*panel B*), a positive control mouse injected with anti-platelet IgG (*panel C*), and a mouse injected with anti-PPARγ-19mer (*panel D*). The bars in *panels B-D* represent 50 μm. The arrows in *panels B-D* denote spleen megakaryocytes.